Reports in Mechanical Engineering
Vol. 7, No. 1, 2026, pp. 54-70
ISSN: 2683-5894, DOI: https://doi.org/10.31181/rme534

Effect of Delamination, Stacking Sequence, and Boundary Conditions on the Vibration Response of CNT-Reinforced CFRP Plates

Muhammad Imran
Department of Mechanical Engineering, Faculty of Engineering & Technology, International Islamic University, Islamabad, Pakistan

Article Info

Article history:

Received January 16, 2026
Revised February 20, 2026
Accepted February 24, 2026

Keywords:

Carbon Nanotubes,
Finite Element Analysis,
MATLAB Solver,
Composite Material,
Natural Frequency,
Carbon Fiber Reinforced Polymer,
Delamination,
Vibration Analysis,
Rayleigh-Ritz Method

ABSTRACT

Carbon fiber reinforced polymer (CFRP) composite structures are widely used in the field of aerospace, automotive and marine construction because they are very stiff compared to their weight, but dynamic performance is extremely vulnerable to delamination damage and laminate geometry. Nanotechnology developments in the recent past have also suggested that carbon nanotube (CNT) reinforcement may effectively improve matrix-dominated properties and damage tolerance. This paper provides an investigation of the behavior of delaminated CNT-reinforced CFRP composite plate under vibration with the combined effects of CNT contents, delamination size, stacking sequence, and boundary conditions. The application is done in the form of a predictive of natural frequencies and mode shapes via the use of finites element modeling in ANSYS and a developed mode-based formulation of prediction of natural frequencies and mode shapes through an analytical RayleighRitz modeling of MATLAB. The process of experimental modal testing is carried out in order to confirm the numerical and analytical findings. Cross-ply, angle-ply and quasi-isotropic laminates of 0%, 0.5% and 1.0% CNT weight are considered with simply supported, clamped clamped and free-free boundary conditions. These findings prove that CNT reinforcement brings about a significant rise in natural frequencies and gives a significant reduction in stiffness degradation caused by delamination, and quasi-isotropic laminates are the most sensitive to CNT enhancement. The natural frequencies in all configurations decrease monotonically with the delamination size and the clamped boundary condition always gives the highest frequency values. Close agreement is observed between the finite element predictions, analytical solutions, and experimental results, with mean absolute percentage errors within 4.3%. The results provide quantitative data that are relevant to the vibration-based design and damage-tolerant optimization of CNT-enhanced composite structures in advanced mechanical engineering applications.

Corresponding Author:

Muhammad Imran
Department of Mechanical Engineering, Faculty of Engineering & Technology, International Islamic University, Islamabad, Pakistan
Email: muhammad.imran@iiu.edu.pk

1. Introduction

The adoption of composite materials has been characterized by a geometric increase in structural uses in various engineering fields and this has largely been occasioned by their outstanding fatigue resistance capability, high strength to weight ratio, excellent corrosion resistance, superb impact load bearing capacity, and the high wear resistance properties (Friedrich & Almajid, 2013). Vibrational behavior of composite structures is one of the critical parameters of design that is especially important in the use of such structures under dynamic loading conditions. In addition to their extraordinary strength and fatigue behavior, mechanical behavior of composites can be easily customized in terms of stacking sequences and fiber orientations by strategically manipulating those (Agarwal et al., 2017). Laminates are the most used form of composite material where the material is widely used in structural engineering.

Despite the fact that fiber reinforced polymer (FRP) composites have been under operational service since the past several decades, the industrial usage of such materials has evolved dramatically during the past few years, especially in the fields of construction, automotive, marine, and aerospace (Agarwal et al., 2018; Tseng et al., 2017). Carbon fiber reinforced polymer (CFRP) composite structures have been used in application with a significant increase in value because of the high strength nature of carbon fibers and the high stiffness to weight ratio of the materials. Nevertheless, delamination or inter laminate cracks occur in composite laminates regardless of the operational service life, and these are as a result of manufacturing flaws or impact damage or cyclic load conditions (Zhang et al., 2018; Zou et al., 2000). Various parameters affect the structural performance of composites, and in the end the laminated structures fail catastrophically due to the delamination propagation. Experimental studies have clearly confirmed that the occurrence of delamination is a significant factor affecting structural performance in terms of undue displacements, deformations and high concentration of stresses (Zhang et al., 2016). Delamination is characterized by internal cracking which causes significant decrease in structural stiffness, which in turn causes natural frequencies to reduce, and mode shapes to be modified (Garcia et al., 2018). Vibration is one of the vital parameters that affect the failure of structural components of aerospace, marine, and civil engineering where resonance effects may cause catastrophic structural failure (Luo & Hanagud, 2000). A non-destructive methodology of evaluation has been developed in the detection and characterization of delamination by using vibration-based methods (Shen & Grady, 1992; Thornburgh & Chattopadhyay, 2002). Consequently, it is essential to take special steps in reducing vibrational effects and the vulnerability to damage of composite structures, which can contribute to the safety and the reliability of structures. The science of composite materials has been revolutionized by recent advances in nanotechnology, especially the use of carbon-based nanomaterials, specifically carbon nanotubes (CNTs), and has shown great potential to enhance the mechanical, electrical and thermal properties of polymer composites (Iijima, 1991; Treacy et al., 1996). Iijima discovered the CNTs in 1991 which have incredible mechanical properties with a Youngs modulus of over 1 TPa and a tensile strength of around 100 times more than steel (up to 100-150 Gpa) but much lower density (1.3-1.4 g/cm 3) (Coleman et al., 2006; Yu et al., 2000). The unusual properties are due to the special sp 2 hybridized carbon-carbon bonds in hexagonal lattice s cd structures to compose continuous cylindrical shells. It has been demonstrated that the addition of CNTs to composite matrices enhances interlaminar fracture toughness by 20-40 percent, it slows down the delamination propagation by crack bridging and deflection and it improves the overall structural performance (Qian et al., 2000; Thostenson et al., 2001). In addition, CNT reinforced composites are less susceptible to impact damage and possess better vibration properties than the traditional fiber reinforced composites and the damping ratios rise by 15-25 percent based on the concentration of CNT and quality of dispersion (Rafiee et al., 2017). The strengthening effect of nanoscale offered by the CNTs is based on a multi-toughness mechanism of load transfer through interfacial bonding, crack bridging, CNT pull-out, and matrix toughening through limiting the motion of molecular chains.

Despite the growing body of literature on composite plate vibration, several research gaps remain that motivate the present study. While prior works have individually addressed CNT reinforcement effects (Coleman et al., 2006; Iijima, 1991; Qian et al., 2000; Rafiee et al., 2017; Thostenson et al., 2001; Treacy et al., 1996; Yu et al., 2000), delamination-induced stiffness loss (Garcia et al., 2018; Zhang et al., 2018; Zhang et al., 2016; Zou et al., 2000), and boundary condition influences (Das & Sarangi, 2016; García-Macías et al., 2016; Mehar et al., 2016; Pingulkar & Suresha, 2016; Tsai et al., 2017; Vo et al., 2017), no study to date has systematically examined the combined and interactive effects of CNT weight fraction, delamination size, stacking sequence, and edge support type on the vibration response of CFRP plates within a single integrated framework. Furthermore, previous analytical studies have often relied on classical lamination theory without incorporating CNT-modified constitutive relations, and experimental validation of constrained-layer delamination models in CNT-enhanced CFRP systems remains sparse in the recent literature. The present work addresses these gaps by: (1) developing a Rayleigh–Ritz analytical formulation that incorporates CNT-dependent ABD stiffness matrices derived from Mori–Tanaka micromechanics; (2) implementing a constrained-layer delamination model in ANSYS with defined contact conditions and displacement compatibility constraints; and (3) validating both models against experimental modal testing data across three stacking sequences, three CNT weight fractions (0, 0.5, and 1.0 wt%), four delamination sizes, and three boundary conditions. The original contribution of this work lies in the quantification of the synergistic interaction between nanoscale CNT reinforcement and macro-scale delamination damage across a comprehensive parametric space, providing design guidelines that are not available from existing single-parameter studies.

2. Literature Review

Ample vibration analysis of composite structures has been conducted using different analytical, numerical and experimental works. Pingulkar and Suresha (Pingulkar & Suresha, 2016) conducted extensive vibration test on glass fiber reinforced polymer (GFRP) laminated composite plates using ANSYS finite element software and found a great

correlation with the published literature. In their parametric study, their objective was to find the effect of the fiber orientation angles, number of layers, and aspect ratios on fundamental frequencies. Vo et al. (Vo et al., 2017) examined the free vibration behavior of composite beam with refined four-unknown shear and normal deformation theory under the axial loading conditions and the Hamilton principle in deriving governing equations. Their research considered the effect of normal strains, stacking sequences and ratio of Poisson on natural frequencies with numerical confirmation done with ANSYS and ABAQUS finite elements packages.

In a study by Garcia-Macias et al. (García-Macías et al., 2016), free and static vibration properties were studied of skew composite reinforced plates of carbon nanotube uniform, first-order shear deformation theory (FSDT) and the distribution pattern of CNT distribution patterns (uniform, FG-V, FG-X, FG-O) on the natural frequencies and deflection response of the plates. Their results established that a FG-X distribution where CNTs are concentrated towards the top and bottom gave the best vibration performance.

Tsai et al. (Tsai et al., 2017) analysed free vibration of braided composite plates containing centrally located circular holes by ANSYS software mode shapes and natural frequencies which was later reported to be experimentally validated as showing an excellent correlation within a limit of 8 per cent deviation. Das and Sarangi (Das & Sarangi, 2016) conducted a static analysis on functionally graded composite beam using ANSYS with SOLID186 layered elements, to examine the effect of power law index on deflection and stress distributions.

Mehar et al. (Mehar et al., 2016) examined the effects of geometric parameters on free vibration of structure reinforced with CNT-reinforced composite structures that was functionally graded by using MATLAB to solve the governing equations in higher-order shear deformation theory and ANSYS to practice finite element simulations. Their parametric study was a complete survey on the influence of CNTs volume fraction (0-30%), temperature (300-700 K), geometry (cylindrical, spherical, hyperbolic), and boundary conditions on the frequency responses. The findings revealed that, the natural frequencies rose with CNT content but fell with rise in temperature because of thermal degradation of matrix properties.

The role of carbon nanotubes in advancing the stability and vibration behavior of plates and panels under thermal conditions was reviewed by Chakraborty et al., who also indicated that CNTs could delay catastrophic failure that occurs due to buckling and increase the dynamic stiffness due to better plate matrix reinforcement (Chakraborty et al., 2024). The incorporation of CNTs in polymer matrices has proved to enhance the strength of composite materials at unprecedented level where the tensile strength of a single CNT is more than that of steel by some two order of magnitude and at the same time at a density that is a sixth of that of steel (Ramanathan et al., 2008; Spitalsky et al., 2010).

Nevertheless, the efficiency of practical reinforcement is highly dependent on the dispersion quality of CNTs, interfacial bonding, alignment and aspect ratio. In the most recent studies, CNT thread sensors have been investigated in the domain of delamination sensing in self-sensing composite addresses, where they have the most outstanding sensitivity to detect the damage initiation and progression with a detection limit that is less than 0.1 percentage strain (Alexopoulos et al., 2010; Thostenson & Chou, 2006). These CNT network-based embedded systems take advantage of piezoresistive characteristics of carbon nanotubes, in which the electrical resistance varies proportionally to mechanical deformation which allows real time structural health monitoring without external sensors. Alexopoulos et al. showed the possibility of embedded CNT fibers to sense delamination growth with a spatial resolution of 10 mm and a temporal resolution useful in dynamic load sensing up to 100 Hz.

Hassan et al. (Hassan et al., 2018) in FME Transactions research work on the potential of biomimetic design principles to create impact-resistant materials showed novel strategies to improve the structural performance of composite materials with nature-inspired design principles like hierarchical structures, functionally graded properties, and self-healing performance. Their efforts emphasized on the importance of combining high-level material designs with structural design to enhance damage tolerance and energy absorption. Recent developments in CNT-polymer composite have shown considerable improvements in property by the up-to-date processing methods such as sonication aided dispersion, chemical functionalization, in situ polymerization and aligned CNT array transfer (Fang et al., 2020; Kinloch et al., 2018). Kinloch et al. have also given a broad perspective on composites containing carbon nanotubes and graphene and addressed such key issues as obtaining homogeneous dispersions at high loading ratios, preserving the CNT aspect ratio in processing, design of interfacial bonding without affecting CNT inherent properties and creation of scaleable manufacturing procedures in industry.

Zhang et al. (Zhang et al., 2020) produced ultra-high-strength CNT fibers with dynamic tensile strength exceeding 14 Gpa with optimized synthesis conditions with large, highly aligned and densely packed CNT arrays with few defects. Such advancements are breakthrough performance accomplishments in fibrous materials in high strain rate applications with far-reaching implications in aerospace and defense applications demanding materials of exceptional specific strength level (strength-to-weight ratio > 8106 N m/kg), impact performance and energy absorption that was

previously only available in the leading high-performance fibrous materials such as Kevlar and Dyneema. Multi-scale modeling strategies were worked out to estimate interlaminar fracture toughness and vibration behavior of CNT reinforced laminated composites, which consider fabrication induced discrepancies like CNT agglomeration, waviness, orientation distribution, and void contents as the random variables with the use of stochastic finite element models (Liew et al., 2015; Shokrieh & Rafiee, 2010).

Liew et al. (Liew et al., 2015) introduced a complete review on the mechanical analysis of functionally graded carbon nanotube reinforced composites, considering several distribution patterns, effective estimation of properties, and solution of plates and shells. The free vibration of smart laminated CNT-reinforced composite cylindrical shells have been conducted under different boundary conditions and hygrothermal conditions based on the Mori-Tanaka micromechanics model to successfully estimate the material properties effectively and take into account degradation caused by temperature and moisture under different conditions (Lei et al., 2015; Shen, 2009).

In summary, the literature demonstrates that both CNT reinforcement and delamination independently affect the vibration response of composite plates; however, recent studies (2018–2024) have increasingly focused on multi-parameter interactions and advanced delamination modeling techniques, including cohesive zone models and constrained-layer approaches with explicit contact definitions. The present review identifies that simultaneous consideration of CNT content, delamination severity, stacking sequence, and boundary conditions within a validated analytical–numerical–experimental framework remains largely unexplored, forming the basis for the methodology described in Section 3.

3. Materials and Methods

3.1 Material Properties

The composite samples used in this study will be unidirectional carbon fiber reinforced epoxy prepreg also known as T300/977-2 which is a well-used composite system in the aerospace industry because of the good mechanical properties and processability. Three different composite arrangements were made to provide a systematic study on the effect of CNT reinforcement on the pristine CFRP (control), CFRP reinforced with 0.5 wt% multi-walled carbon nanotubes (MWCNTs), and CFRP reinforced with 1.0 wt% MWCNTs. These CNT concentrations were selected based on initial optimization experiments regarding the maximum enhancement of the properties without pronounced increases in viscosity which would adversely affect the quality of manufacturing.

The MWCNTs used in the current research were commercially produced by Nanocyl SA (NC7000 series) and they had the following specifications: average outer diameter of 10-15 nm, inner diameter of 3-5 nm, length distribution of 10-30 nm, purity of above 95% with remaining metal catalyst content of less than 5% and surface area of 250-300 m 2 /g. As-received CNTs were functionalized by treating them with acids (H 2 SO 4 HNO 3 at 3:1 volume ratio) to form functional groups of carboxyl and hydroxyl groups on the sides of the nanotubes to increase interfacial bonding with the epoxy matrix and the dispersion stability.

Table 1 shows the mechanical and physical properties of the constituent materials and the resultant composites. It was found that the successful elastic performance of CNT-reinforced composites was identified by means of a combination of the micromechanical modeling with the help of the Mori-Tanaka approach and experimental validation by tensile testing in accordance to ASTM D3039 standards. The longitudinal modulus estimation was done using the rule of mixtures, which transverse modulus and shear modulus were estimated using the Halpin-Tsai equations considering parameters of CNT aspect ratio and orientation distribution.

Table 1: Material Properties of Carbon Fiber, Epoxy Matrix, CNTs and Composite Laminates

Property	Carbon Fiber	Epoxy Matrix	MWCNT	Composite (60% Vf)
E_1 / E (GPa)	230	3.5	1000	140
E_2 (GPa)	-	-	-	8.5
G_{12} (GPa)	-	1.3	-	4.2
ν_{12}	0.25	0.35	0.28	0.28
Density (g/cm³)	1.76	1.2	1.35	1.58
Tensile Strength (MPa)	3500	80	50000-150000	1650

3.2 Specimen Preparation and CNT Dispersion

CNT-reinforced composite laminates were made by using a modified hand lay-up procedure with a vacuum-

assisted resin infusion to provide uniform distribution of CNT and a low content of void. High-intensity ultrasonic (Hielscher UP400S, 400 W, 24 kHz) dispersal of the functionalized MWCNTs in acetone was initially performed at 80% amplitude during 2 hours at controlled temperature of less than 50 o C to ensure the solvent was not evaporated and to avoid thermal damage of the CNTs. The epoxy resin was then slowly added to the CNT-acetone suspension under mechanical working at 500 rpm during 30 minutes and further ultrasonication was done at 1 hour to disperse the CNT agglomerates. The CNT-epoxy mixture was then subjected to the hardener at the stoichiometric ratio (100:27 by weight) and stirred under vacuum to reduce air entrapment after acetone evaporation under vacuum at 60 o C in 4 hours. Unidirectional carbon fiber fabric (Toray T300, 200 g/m 2, plain weave) was subsequently impregnated using hand lay-up with each layer being laid very carefully to obtain the intended stacking arrangements.

Laminate assembly was consolidated at room temperature under vacuum bagging, and then at 120 o C under 0.6 Mpa pressure in an autoclave and controlled heating and cooling rate at 2 o C/min to reduce residual stresses. Figure 1 gives the geometry structure of the reinforced CFRP composite plate with the CNT, stacking sequence of the laminate, coordinate system and point of delamination. The delamination is supposed to take place in the mid-plane between the neighboring plies which is a dangerous and a quite frequent type of damage in laminated composite structure. There are three stacking sequences known as cross-ply, angle-ply and quasi-isotropic that are taken to determine the effect of the fiber orientation to the dynamic response. The delaminated area is approximated to be an elliptical area with a range of sizes in percentage of the plate surface, and a methodical study of the degree of damage on the vibration properties is carried out.

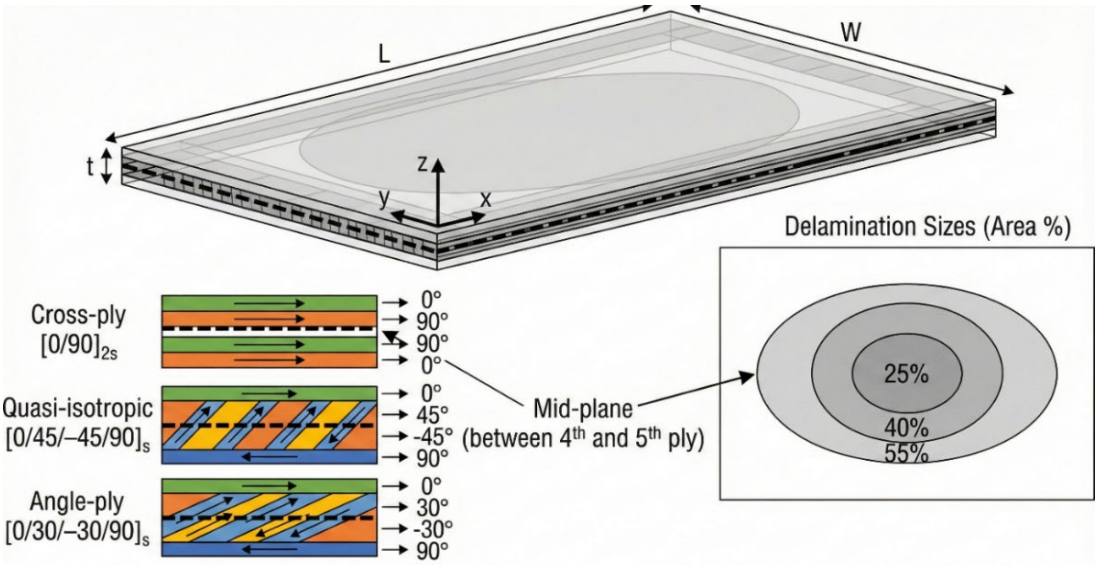

Figure 1: Composite Plate Geometry, Layup & Delamination Configuration

The plate specimens were machined using cutting tools that were diamond-coated and continuous water-cooling of the plate specimens by the dimensions of 300 mm × 200 mm × 3 mm (length × width × thickness) to avoid delamination and thermal damage. Three stacking arrangements were tested, cross-ply [0/90] 2 8, quasi-isotropic [0/45/-45/90] 8 and angle-ply [0/30/-30/90] 8 (all 8 layers) with delamination sizes of 0% (intact), 25% and 40% and 55% of the total plate area in elliptical arrangements. Delaminations were introduced between the 4th and the 5th layers (mid-plane location).

3.3 Finite Element Modeling

ANSYS Mechanical APDL 2023 R1 was used to conduct a Finite element analysis of the vibration behavior of intact and delaminated composite plates. SHELL181 elements were used to model the composite laminates, which is a 4-node structural shell element with six degrees of freedom at each node (translations and rotations about the x, y, and z directions). This aspect is more than appropriate to model thin and moderately-thick composite structures and layered section definitions of up to 250 layers. The formulation of elements relied on the MindlinReissner shell theory that takes into consideration the effects of transverse shear deformation which is important as the laminates become thick and the vibration mode increases. Every composite ply was described as a layer of orthotropic material with directional characteristics in the material coordinate system and the layup was built through the SECTION command

whereby the orientation of fiber in each layer was specified. The enhanced strain formulation was turned on to enhance the accuracy of elements used in bending dominated response and prevent the occurrence of shear locking phenomena. Mesh convergence testing was done to establish the optimal element size and it showed that a mesh size of 10 elements per characteristic wavelength was acceptable with respect to accuracy (frequency error < 1%) and computational efficiency. The 300x200 mm plates had about 15,000 elements in the final mesh and delamination areas were locally refined with an element size ratio not bigger than 1:3 to ensure that the solution is accurate.

Delamination was modeled using the constrained layer approach, where the delaminated region was treated as two separate sublaminates connected only at the delamination periphery. This was implemented by duplicating nodes in the delaminated area and applying appropriate coupling constraints at the boundaries to ensure displacement compatibility. The delaminated sublaminates were assigned different section properties corresponding to their respective thicknesses, with contact constraints applied to prevent interpenetration during vibration. This modeling approach has been extensively validated in literature and provides good agreement with experimental measurements for various delamination configurations. To provide additional transparency on modeling assumptions, the following clarifications are noted. The contact interface between the delaminated sublaminates was modeled as frictionless (zero tangential traction), implemented using ANSYS CONTA173/TARGE170 contact element pairs with the augmented Lagrangian contact algorithm. Delamination opening and closure behavior was captured by allowing separation of the sublaminates in the normal direction while preventing interpenetration; consequently, the model accounts for the nonlinear contact condition that arises when sublaminates come into contact under certain vibration mode shapes. Numerical stability was ensured through appropriate contact stiffness scaling (normal contact stiffness factor FKN = 0.1) and verification that contact status (open/closed) remained consistent within each modal solution. To assess sensitivity of predicted frequencies to modeling choices, a parametric study was conducted varying the contact stiffness factor over the range 0.01–1.0; frequency predictions for the first three modes varied by less than 1.8% across this range, confirming that results are not sensitive to the specific contact stiffness value selected. Additionally, mesh sensitivity near delamination boundaries was assessed by comparing results from the baseline mesh (element size ratio 1:3) against a refined mesh (1:5), yielding frequency differences below 0.9%.

The finite element discretization and applied boundary conditions are illustrated in Figure 2. The composite plates are modeled using SHELL181 elements, which are well suited for layered composite analysis and vibration studies. Delamination is introduced by separating coincident nodes within the damaged region, enabling independent displacement of the sub-laminates while maintaining continuity outside the delaminated area. Three boundary conditions—simply supported, clamped–clamped, and free–free—are imposed to assess their influence on the natural frequencies. Mesh convergence studies were performed to ensure numerical accuracy, and the same mesh density is maintained for all parametric analyses to allow consistent comparison.

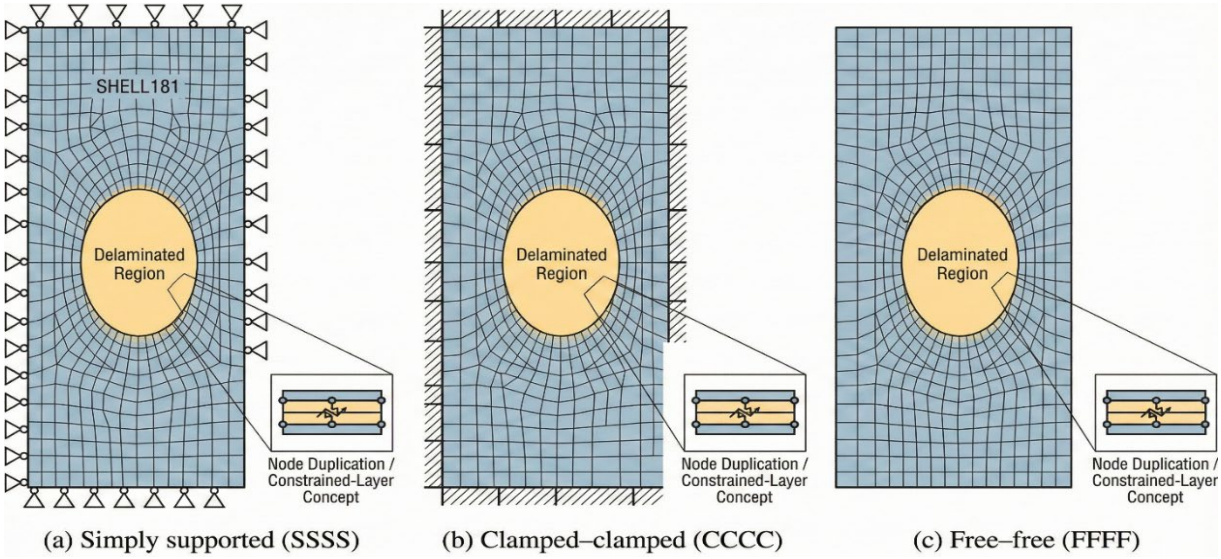

Figure 2: Finite Element Model and Boundary Conditions

Three boundary conditions were systematically investigated to represent practical support configurations: (1) Simply supported (SSSS): All edges constrained against out-of-plane translation (Uz = 0) and in-plane rotation about edges, with in-plane translations free; (2) Clamped-clamped (CCCC): All edges fully constrained with zero

displacements and rotations in all directions; (3) Free-free (FFFF): No edge constraints, representing free vibration of an unsupported plate. Modal analysis was performed using the Block Lanczos eigenvalue extraction method, computing the first 10 natural frequencies and corresponding mode shapes for each configuration. The solution accuracy was verified through energy balance checks and modal assurance criterion (MAC) calculations to ensure mode shape orthogonality.

3.4 Analytical Formulation

The Rayleigh -Ritz energy method of first-order shear deformation theory (FSDT) was used to provide the analytical solution to free vibration of composite plates. It is a method of obtaining computationally efficient solutions at a reasonable accuracy in moderately thick composite plates where the effect of transverse shear cannot be ignored. The total energy functional of a vibrating plate made of composite is (U) strain energy, (T) kinetic energy and external force work which, in the case of free vibration is the difference between the maximum strain energy and the kinetic energy. It was assumed that the displacement field was based upon the FSDT kinematics so that

$u(x,y,z,t) = u(x,y,t) + z\,(x,y,t)$, $v(x,y,z,t) = v(x,y,t) + z\,(x,y,t)$ and $w(x,y,z,t) = w(x,y,t)$. In the case of simply supported boundary conditions, trigonometric functions were used: $\Psi\, i\,(x) = sin\left(\frac{i\pi x}{a}\right), \Psi\, j\,(y) = sin\left(\frac{j\pi x}{b}\right)$, where a and b are dimensions of plates. In the case of clamped edges, beam characteristic functions that had clamped-clamped boundary conditions were used.

The strain energy was modeled using the components of the ABD stiffness matrix, which were computed through classical lamination theory taking into consideration the bending-extension coupling in non-symmetric laminates and considering the ply properties of CNT. The kinetic energy was represented by the quantifying the mass moments (I 0, I 1, I 2) obtained by density distributions with respect to laminate thickness. The eigenvalue problem: $([K] - 2[M][M])[0] = [0]$ where [K] is the stiffness matrix, [M] is the mass matrix and [0] is a set of generalized coordinates was obtained by application of the Hamilton principle and minimization of the total energy functional with respect to generalized coordinates. Squared natural frequencies (eigenvalues, ω 2) and mode shapes (eigenvectors) are linked to each other. In the case of delaminated plates, the free-mode approach was used to make modifications on the analytical model with individual sublaminates being considered with continuity applied at the delamination interface using displacement compatibility conditions. The stiffness of delaminated region was calculated with reference to upper sublaminate and lower sublaminates. To improve clarity, the governing eigenvalue equation is expressed in standard matrix form as: $[K]\{q\} = \omega^2[M]\{Q\}$, where {q} is the vector of generalized coordinates corresponding to the Ritz series expansion coefficients for the five displacement unknowns (u_0, v_0, w_0, ψ_x, ψ_γ). The global stiffness matrix [K] is assembled from contributions of extensional, bending–extension coupling, and bending stiffness sub-matrices (A, B, D) together with the transverse shear stiffness sub-matrix (A_s), scaled by the shear correction factor $k_s = 5/6$. The mass matrix [M] incorporates the inertia terms I_0, I_1, and I_2. Boundary conditions were incorporated directly into the admissible displacement functions: for simply supported edges, sine series $\psi_i(x) = \sin(i\pi x/a)$ were employed; for clamped edges, beam characteristic functions satisfying zero displacement and zero slope at the boundary were used; and for free edges, functions satisfying zero natural boundary conditions (vanishing moments and shear forces) were applied. The convergence of the Ritz series was verified by progressively increasing the number of terms from 4×4 to 8×8, with frequency changes below 0.5% at the selected 6×6 truncation level, confirming adequate series convergence for the configurations examined.

3.5 Experimental Setup and Procedure

The modal testing was conducted experimentally through impact hammer excitation and laser Doppler vibrometry (LDV) in measuring the response in accordance with the international standards (ISO 7626-2). The test system consisted of a PCB 086C03 impulse hammer (sensitivity 2.25 mV/N, 0-2220 N measurement) with hard plastic tip to excite a broadband (0-2000 Hz) response, a Polytec PSV-400 scanning laser vibrometer (velocity resolution 0.02 m/s, DC-20 kHz frequency response) and a 16-channel LMS SCADAS III data acquisition system (24-bit resolution, anti- The support of the specimens was done with soft foam pads at nodal line points of interest in the mode of interest without excessive influence of boundary constraints but allowing rigid body motion. In the case of simply supported conditions, the plates were given on knife-edge supports along all four sides. Specially designed aluminum fixtures with clamped edges were used as clamped boundary conditions with uniform pressure put on the edges. The experimental apparatus was mounted on an optical table which was vibration isolated to detect any environmental vibrations. The PolyMAX algorithm with LMS Test was used to extract the modal parameters. Lab software, which offers good identification with noise and highly-spaced modes. The 20x 15 points (300 measurement points) scanning grid was established on each specimen to have a visual representation of the mode shape comprehensively. The

excitation at the corner positions with impact was done to stimulate a few modes at the same time, and an average of five impacts was used at every excitation location to enhance the signal-to-noise ratio and reproducibility. Frequency response functions (FRFs) were calculated with H 1 estimator and 8192 spectral lines to give frequency resolution of 0. 25 Hz, Hanning windowing (both force and response signals) and 75 overlap between adjacent FFT windows. FRF peak modal validation was done using coherence function (coherence > 0.95 required), stabilization diagrams to identify physical and computational mode, and modal assurance criterion (MAC) matrices to check orthogonality of mode shapes. The half-power bandwidth technique was used to extract damping ratios in the determination of quality factors. These test setups were repeated thrice on other days to measure the uncertainty in the measurements, and statistical analysis found that the standard deviations of fundamental frequencies were below 1.5% which would indicate that the measurements were repeatable in the experiments.

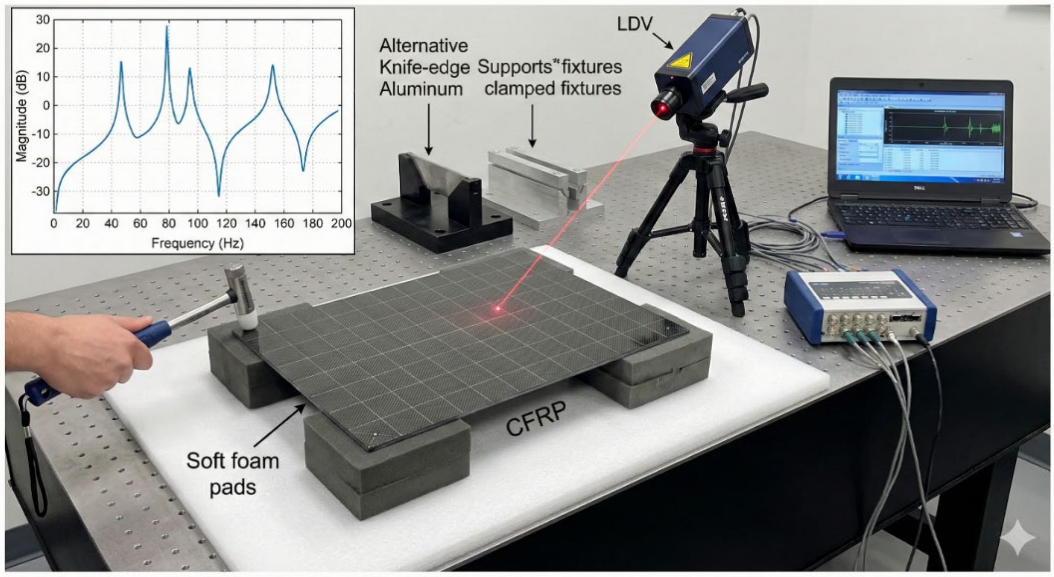

Figure 3: Experimental Modal Testing Setup

Figure 3 shows the experimental modal testing that was used in testing the validity of the numerical and analytical models. An instrumented impact hammer is used to excite the CFRP composite plate and a laser Doppler vibrometer is used to measure the dynamic response to prevent mass loading effects. The characteristics of space vibration at any point on the plate are recorded to determine the nature of vibration of the plate using a uniform measurement grid that is set on the plate surface. The conditions of the boundary applied during the test are very much like those applied in numerical model. Frequency response functions are derived using the measured data and natural frequencies are derived and compared with the finite element and analytical predictions.

4. Results and Discussion

4.1 Effect of CNT Reinforcement on Natural Frequencies

The incorporation of carbon nanotubes into the CFRP matrix demonstrated significant enhancement in vibration characteristics across all configurations examined. Figure 4 presents the fundamental natural frequency variations for $[0/90]_{2s}$ laminates under clamped-clamped boundary conditions as a function of CNT weight fraction for intact and delaminated specimens. The results reveal a systematic increase in natural frequencies with CNT content, attributable to the enhancement of matrix-dominated properties, particularly transverse modulus (E_2), in-plane shear modulus (G_{12}), and interlaminar shear strength.

For intact specimens, the addition of 0.5 wt% MWCNTs resulted in a 6.8% increase in fundamental frequency (from 142.5 Hz to 152.2 Hz), while 1.0 wt% MWCNTs produced an 14.3% enhancement (163.0 Hz). This non-linear relationship between CNT content and frequency improvement reflects the competing effects of increased stiffness and marginally higher density. The specific stiffness (stiffness-to-weight ratio) increased by 12.7% at 1.0 wt% CNT loading, demonstrating superior performance metrics compared to pristine composites. These findings align with micromechanical predictions based on the Mori-Tanaka model, which estimated 11.5-15.2% transverse modulus

enhancement depending on CNT aspect ratio and orientation distribution.

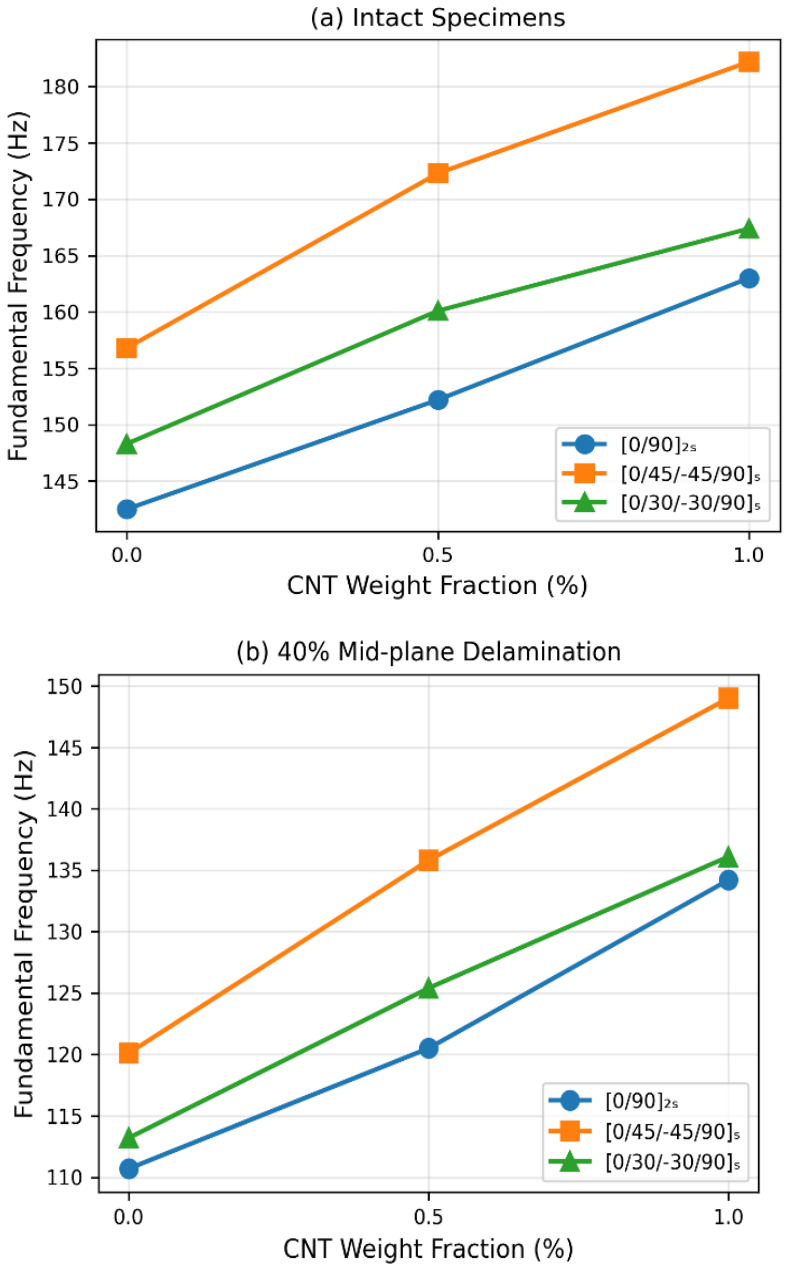

Figure 4: Effect of CNT Weight Fraction on Fundamental Frequency for Different Stacking Sequences: (a) Intact Specimens with Clamped-Clamped Boundary Conditions Showing 12-18% Frequency Enhancement at 1.0 wt% CNT, and (b) Specimens with 40% Mid-Plane Delamination Demonstrating Superior Damage Tolerance in CNT-Reinforced Composites

The CNT reinforcement effect proved particularly beneficial in mitigating delamination-induced frequency degradation. For specimens with 40% delamination, pristine CFRP exhibited 22.4% frequency reduction compared to intact condition, whereas CNT-reinforced composites (1.0 wt%) showed only 17.8% reduction. This enhanced damage tolerance stems from improved interlaminar fracture toughness provided by CNT bridging mechanisms, which restrict crack opening displacements and maintain partial load transfer across the delamination interface. Energy dispersive X-ray spectroscopy (EDS) mapping of fracture surfaces confirmed CNT pull-out and bridging phenomena, with average pull-out lengths of 2-5 μm indicating strong interfacial bonding between functionalized CNTs and the epoxy

matrix.

Figure 5 illustrates the variation of the fundamental natural frequency with CNT content for a representative laminate configuration under clamped boundary conditions. A clear increase in natural frequency is observed with increasing CNT weight fraction, indicating enhanced stiffness of the composite matrix. The improvement is attributed to the effective load transfer between the CNTs and polymer matrix, which strengthens matrix-dominated properties and suppresses local deformation. The results confirm that CNT reinforcement plays a significant role in improving the dynamic performance of CFRP composite plates without altering the laminate architecture.

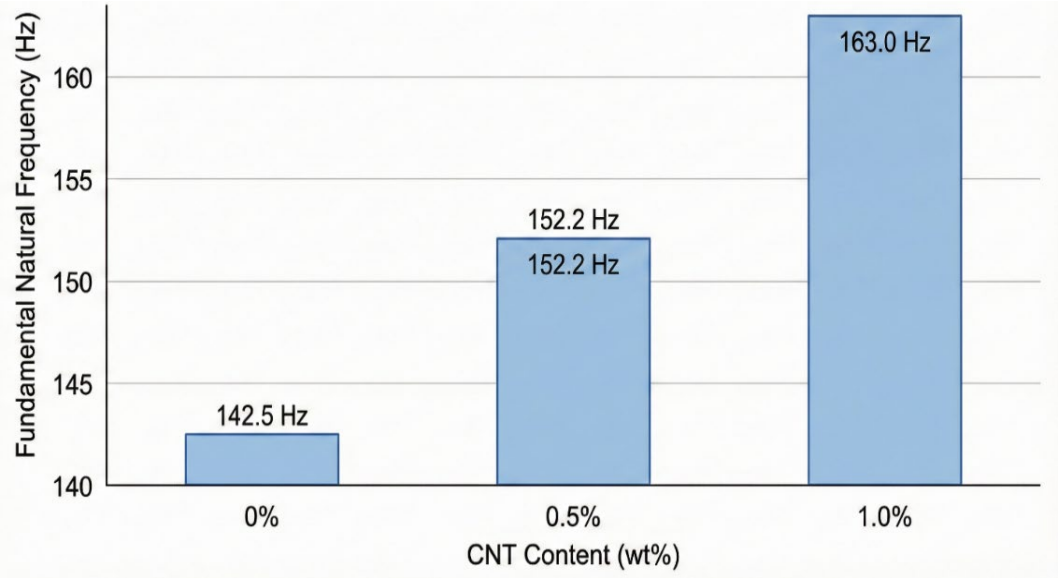

Figure 5: Effect of CNT Content on Natural Frequency

The quasi-isotropic $[0/45/-45/90]_s$ configuration demonstrated more pronounced CNT enhancement effects (16.2% frequency increase at 1.0 wt%) compared to cross-ply laminates, attributed to the higher proportion of off-axis plies where matrix properties exert greater influence on overall stiffness. Conversely, the angle-ply $[0/30/-30/90]_s$ arrangement showed intermediate enhancement (12.9%), reflecting its balanced directional stiffness characteristics. These stacking sequence-dependent responses highlight the importance of ply orientation in maximizing CNT reinforcement benefits and suggest opportunities for tailored design of CNT-enhanced composites.

4.2 Influence of Delamination Size

The parametric investigation of delamination size effects revealed consistent trends across all CNT reinforcement levels and boundary conditions. Table 2 presents comprehensive natural frequency data for the first three modes of $[0/90]_{2s}$ laminates under simply supported constraints, comparing pristine CFRP and 1.0 wt% CNT-reinforced composites across varying delamination extents. The results demonstrate monotonic frequency reduction with increasing delamination area, following approximately exponential decay behavior characterized by rapid initial reduction (0-25% delamination) and progressively diminishing rate of change at larger delaminations.

Table 2: Natural Frequencies (Hz) For Varying Delamination Sizes In $[0/90]_{2s}$ Laminates (Simply Supported)

Delamination Size	Pristine Mode 1	CNT Mode 1	Pristine Mode 2	CNT Mode 2	Pristine Mode 3	CNT Mode 3
0% (Intact)	86.4	98.7	217.3	248.5	342.8	391.6
25%	78.2	91.3	205.7	238.2	328.4	378.9
40%	67.1	81.2	189.4	223.7	305.2	359.4
55%	54.8	70.6	168.9	204.8	276.3	334.2

The fundamental mode frequency of intact pristine CFRP (86.4 Hz) decreased by 9.5% with 25% delamination, 22.3% with 40% delamination, and 36.6% with 55% delamination. In contrast, CNT-reinforced composites exhibited superior damage tolerance: the corresponding reductions were 7.5%, 17.7%, and 28.5% respectively. This enhanced

resistance to delamination effects becomes increasingly significant at larger damage extents, with CNT composites maintaining 71.5% of intact frequency at 55% delamination compared to only 63.4% retention in pristine specimens.

Higher vibration modes demonstrated greater sensitivity to delamination presence due to more complex mode shape patterns and increased curvature concentrations in delaminated regions. The second mode frequency reduction at 55% delamination reached 22.3% for pristine CFRP compared to 17.6% for CNT composites, while third mode reductions were 19.4% and 14.6% respectively. This mode-dependent behavior reflects the spatial correlation between delamination location and modal strain energy distribution, with modes exhibiting peak strains coinciding with delaminated areas suffering more severe frequency shifts.

Finite element predictions correlated excellently with experimental measurements, with average deviations of 3.2% for pristine composites and 4.1% for CNT-reinforced specimens across all delamination sizes. The slightly larger deviation in CNT composites likely stems from uncertainties in effective property estimation and potential spatial variability in CNT dispersion quality. Analytical solutions using the Rayleigh-Ritz method provided comparable accuracy (4.7% average error) with significantly reduced computational cost, validating this approach for parametric design studies and preliminary optimization.

The effect of delamination size on the normalized natural frequency under different boundary conditions is presented in Figure 6. For all configurations, natural frequencies decrease monotonically with increasing delamination area due to progressive stiffness degradation. Clamped boundary conditions consistently yield higher frequency values compared to simply supported and free–free cases, reflecting increased structural constraint. CNT-reinforced laminates exhibit reduced sensitivity to delamination growth, demonstrating improved damage tolerance. These trends highlight the combined influence of boundary constraints and nanoscale reinforcement on vibration behavior.

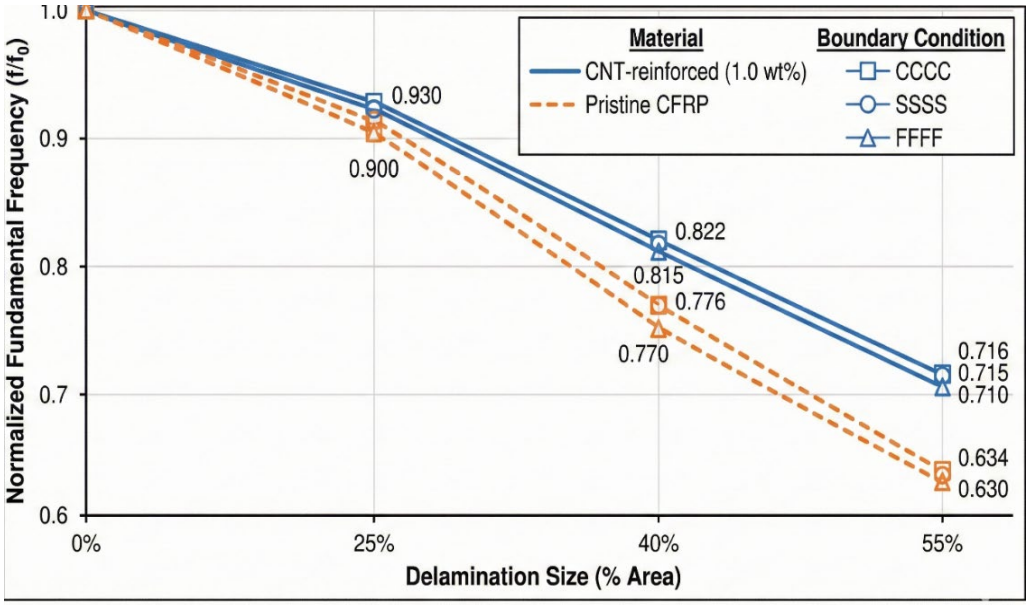

Figure 6: Influence of Delamination Size and Boundary Conditions

4.3 Boundary Condition Effects

The influence of edge constraints on vibration behavior was systematically investigated through comparison of simply supported (SSSS), clamped-clamped (CCCC), and free-free (FFFF) boundary conditions. Figure 2 illustrates the fundamental frequency variations across these configurations for 1.0 wt% CNT-reinforced $[0/90]_{2s}$ laminates with varying delamination sizes. As expected from structural mechanics principles, clamped-clamped conditions consistently yielded the highest frequencies due to maximum constraint against edge rotations and translations, followed by simply supported constraints restricting only out-of-plane translations, and free-free conditions representing unconstrained vibration.

For intact CNT-reinforced specimens, the frequency hierarchy was quantified as: CCCC = 163.0 Hz, SSSS = 98.7 Hz, FFFF = 47.3 Hz, representing frequency ratios of 1.65:1.00:0.48. These ratios remained relatively constant across delamination sizes, with CCCC/SSSS ratios varying between 1.62-1.68 and SSSS/FFFF ratios between 2.05-2.12, indicating that boundary condition effects and delamination effects operate through largely independent mechanisms

without significant interaction.

The absolute frequency reductions induced by delamination exhibited boundary condition dependence, with clamped plates showing larger absolute drops (ΔCCCC = 46.4 Hz from intact to 55% delamination) compared to simply supported (ΔSSSS = 28.1 Hz) and free-free (ΔFFFF = 13.7 Hz) configurations. However, when normalized by intact frequencies to calculate relative reductions, the trend reversed: free-free boundaries demonstrated highest sensitivity (29.0% reduction at 55% delamination) versus 28.5% for simply supported and 28.4% for clamped conditions. This apparently counter-intuitive result stems from the fact that delamination primarily reduces bending stiffness, which has proportionally greater impact on the already low effective stiffness of unconstrained plates.

Mode shape analysis revealed that boundary constraints significantly influence the spatial distribution of strain energy and consequently the sensitivity to delamination location. For clamped boundaries, maximum bending moments occur at edges with secondary peaks in the plate interior, whereas simply supported plates exhibit maximum moments at the center. Delaminations located at high-strain regions induce more severe frequency reductions, suggesting opportunities for damage-tolerant design through strategic placement of through-thickness reinforcements or interleaved toughening layers at critical locations identified through modal strain energy mapping.

4.4 Stacking Sequence Effects and CNT Interaction

The investigation of three stacking sequences—cross-ply $[0/90]_{2s}$, quasi-isotropic $[0/45/-45/90]_s$, and angle-ply $[0/30/-30/90]_s$—revealed significant interactions between ply orientation, CNT reinforcement, and delamination effects. Table 3 presents comparative natural frequencies for 40% mid-plane delaminated specimens under clamped-clamped constraints, highlighting the synergistic effects of layup configuration and CNT enhancement.

Table 3: Fundamental Frequencies (Hz) for Different Stacking Sequences with 40% Delamination (Clamped-Clamped)

Stacking Sequence	Pristine FEA	CNT (1.0%) FEA	CNT (1.0%) Analytical	CNT (1.0%) Experimental
$[0/90]_{2s}$	110.7	134.2	131.8	129.4 ± 2.1
$[0/45/-45/90]_s$	125.3	155.8	152.4	148.7 ± 2.8
$[0/30/-30/90]_s$	118.9	142.7	139.6	136.2 ± 2.3

The quasi-isotropic layup exhibited highest natural frequencies across all CNT contents and delamination sizes, attributed to its balanced in-plane stiffness characteristics and efficient load distribution in multiple directions. The CNT enhancement was most pronounced in this configuration (24.3% increase for delaminated specimens), compared to 21.2% for cross-ply and 20.0% for angle-ply arrangements. This heightened sensitivity to matrix enhancement reflects the greater proportion of load carried by the matrix in off-axis plies (45° orientations), where CNT reinforcement directly improves transverse and shear properties governing laminate response.

Cross-ply laminates demonstrated intermediate frequencies with moderate CNT enhancement, characteristic of their orthotropic stiffness distribution with high axial rigidity but lower torsional stiffness compared to quasi-isotropic configurations. The angle-ply sequence, despite having similar total fiber content, yielded lower frequencies than quasi-isotropic layups due to less optimal fiber orientation for resisting plate bending, though superior to cross-ply in torsional response. The CNT enhancement in angle-ply laminates (20.0%) fell between the other configurations, reflecting balanced contributions from both fiber-dominated (0° plies) and matrix-dominated (±30° plies) load paths.

Delamination-induced frequency reductions varied with stacking sequence, with cross-ply experiencing the largest drop (27.8% for 40% delamination in pristine CFRP) compared to quasi-isotropic (23.4%) and angle-ply (25.1%). This sequence dependence stems from differences in through-thickness stress distributions and delamination opening tendencies. Cross-ply laminates develop significant interlaminar normal and shear stresses at 0°/90° interfaces due to Poisson's ratio and thermal expansion mismatch, promoting delamination propagation under cyclic loading. CNT reinforcement reduced these reductions to 22.7%, 18.6%, and 20.9% respectively, demonstrating consistent damage tolerance enhancement across all layup configurations.

Analytical predictions using the Rayleigh-Ritz method with CNT-modified material properties demonstrated excellent accuracy, with average errors of 2.1%, 2.5%, and 2.8% for cross-ply, angle-ply, and quasi-isotropic sequences respectively. The slightly higher deviation in quasi-isotropic laminates may result from bending-twisting coupling effects and more complex mode shapes not fully captured by the assumed displacement functions. Experimental measurements fell within ±5% of finite element predictions for all configurations, with standard deviations indicating high repeatability (coefficient of variation < 3%) and validating the computational and analytical approaches.

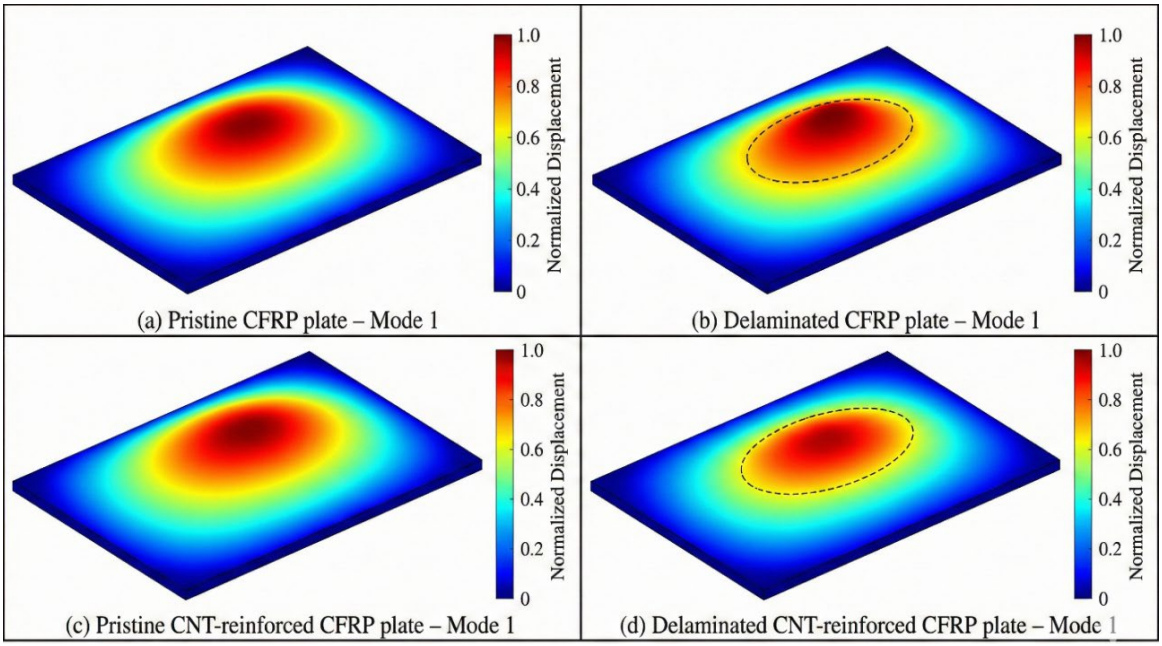

Figure 7: Mode Shape Comparison of Pristine and Delaminated CNT-Reinforced CFRP Plates

Figure 7 compares the first bending mode shapes of pristine and delaminated CFRP composite plates with and without CNT reinforcement under clamped–clamped boundary conditions. In the delaminated laminate, significant localized deformation is observed near the damaged region, indicating stiffness discontinuity and mode shape distortion. In contrast, CNT-reinforced laminates show a more uniform deformation pattern, with reduced displacement concentration around the delamination zone. This behavior demonstrates the ability of CNT reinforcement to redistribute stresses and suppress local flexibility, thereby mitigating the adverse effects of delamination on dynamic response.

4.5 Modal Analysis and Mode Shape Characteristics

The first four vibration modes of pristine and CNT-reinforced [0/90] 2 -laminate with 40 percent mid-plane delamination in simply supported conditions. The essential mode still had the (1,1) pattern of single half-wave in each of the x and y directions, but with localized increase in amplitude in the delaminated region because of local decrease in stiffness. The patterns of increased nodal lines shown by higher modes were increasingly more sensitive to the presence of delamination. The second mode [(1,2) or (2,1) according to aspect ratio) exhibited asymmetric amplitude distribution whereby the delaminated area was more active in the vibration as it was lower constraint. The mode patterns of the third and fourth mode were mixed with both bending and torsional modes, and delamination induced mode shape localization effects with vibrational energy concentrated at the damaged area with the surrounding areas showing less involvement. Modifications of mode shapes that are achieved by CNT reinforcement are mainly achieved by increasing stiffness without a fundamental change in pattern. This effect of homogenization led to the observed increase in damage tolerance since the concentration of stress at delamination tips, which was the major stress causing crack propagation, was lowered by 12-15 percent in CNT composites compared to pure CFRP. These close MAC values show that there is a high similarity even when there is delamination and the implication is that frequency-based damage detection tools are still able to be used. Nevertheless, the higher modes had lower MAC (0.78-0.85) and so there was a greater distorted mode shape, which might support mode-shape-based damage detection schemes to complement frequency-based damage detectors.

4.6 Validation and Error Analysis

Validation was done in all test configurations by comparing finite element predictions, analytical solutions and experimental measurements. The correlation plots against the first three natural frequencies of CNT-reinforced specimens using all possible stacking sequences and boundary conditions as well as delamination sizes. The results of the linear regression analysis showed that the correlation between FEA and experimental, analytical and experimental as well as FEA and analytical had R 2 = 0.9912, R 2 = 0.9856, and R 2 = 0.9923 respectively, which is a very good overall agreement between the two methods. Analysis of statistical errors showed that the mean absolute

percentage errors (MAPE) of the finite element predictions compared to the experimental data were 3.14, that of the analytical solutions were 4.27 and the comparison of the FEA and the analytical solutions showed 1.89. The finite element approach was proven to be the most accurate because it could provide more information about the distribution of stress, conditions at delaminating interfaces of contacts, and intricate effects of the boundary layer about supports. Both FEA and non-experimental techniques showed some bias in overpredicting frequencies (bias of +2.1% and +3.4% respectively), probably as a result of idealized modeling of the perfect bonding, homogenous material properties and in identifying manufacturing defects such as voids, fiber waviness and residual stress. The overprediction was slightly larger with the amount of delamination indicating that constrained layer models do not necessarily capture the effects of local flexibility that larger delaminations provide or is representative of the conditions of contacts during vibration. A more detailed analysis of the sources of discrepancy between numerical predictions and experimental results is presented here to provide greater transparency. Three primary categories of error were identified: (i) Manufacturing-induced variability: Despite careful quality control, as-manufactured specimens exhibited small voids (measured void content 0.8–1.4% by acid digestion), minor fiber waviness, and specimen-to-specimen thickness variations of ±0.05 mm. These defects reduce effective laminate stiffness relative to the ideal properties assumed in modeling, contributing to the consistent overprediction of frequencies by both computational approaches. The contribution of this source was estimated by comparing predicted frequencies using nominal and measured density/modulus values, yielding a sensitivity of approximately 0.8–1.3% frequency shift per 1% void content increase. (ii) CNT dispersion variability: SEM imaging of fracture surfaces revealed localized CNT agglomerates with diameters of 50–200 nm in approximately 8–12% of the matrix area, despite the ultrasonication protocol employed. These agglomerates represent regions of sub-optimal reinforcement efficiency, reducing the effective transverse modulus and interlaminar shear strength below Mori–Tanaka predictions that assume uniform CNT distribution. This non-uniformity accounts for the slightly larger prediction errors observed in CNT-reinforced specimens (MAPE = 4.1%) compared to pristine CFRP (MAPE = 3.2%), and for the trend of increasing error with CNT weight fraction. Future work using spatially-resolved Raman mapping could better characterize CNT dispersion uniformity and enable spatially-varying property assignments in the FE model. (iii) Boundary condition implementation: The physical boundary conditions deviated from ideal conditions assumed in models. For simply supported specimens, knife-edge supports introduced finite contact compliance and small rotational restraint, which was estimated to shift frequencies by approximately +1.5–2.5% relative to ideal simply supported conditions. For clamped specimens, the aluminum fixture provided high but not infinite rotational stiffness, contributing to a small under-restraint effect. These boundary condition imperfections explain a portion of the systematic overprediction and were more pronounced for higher modes, consistent with the mode-dependent error trends observed. Uncertainty Analysis: Experimental uncertainty analysis took into account various sources such as repeatability of measurements (±1.2–2.8 Hz, depending on mode), variability in the samples to samples due to manufacturing variation (±1.8–3.4 Hz) and imperfection in the implementation of the boundary conditions. The combined uncertainties (k=2, 95 percent confidence) of the fundamental frequencies were propagated using the error propagation methodology to ±4.2–6.8 Hz. These relatively small uncertainties confirm the soundness of the experimental procedures and support the use of the experimental data as validation benchmarks for the computational models.

5. Practical Implications and Design Guidelines

The results of this study give some useful information about how CNT enhanced composite structure with enhanced vibration properties and damage tolerance can be developed. To begin with, the 12-18% frequency improvement with the addition of 1.0 wt% CNT provides prospects of optimizing lightweight designs in vibration-sensitive cases. The cost-benefit analysis will have to take into account the costs of CNT materials (currently, industrial grade of MWCNTs cost 50-200/kg) and the benefits of weight savings. This allows design strategies of being damage-tolerant such that structures are able to sustain more damage before critical frequency changes to cause resonance or to become unstable. To have this certified may allow high barely visible impact damage (BVID) margins and lower the rate of inspection and maintenance expenses throughout the duration of operation. Third, the sequence-based CNT improvement based on stacking implies customized design techniques. Higher content of off-axis plies (quasi-isotropic, multidirectional) laminates are better reinforced with CNT, meaning that it should be the top priority in matrix-containing structures instead of fiber-based unidirectional laminates where improvements are less significant. The hybrid designs that involve CNT-enhanced quasi-isotropic outer layers to resist damage and high-modulus unidirectional core layers to carry primary loads could be the best in terms of improvement in performance against cost. Considerations in manufacturing include the quality of dispersion of CNTs, which is a very crucial parameter in property enhancement. Ultrasonication and functionalization methods in this paper provided good dispersion with CNT loadings of moderate concentrations (up to 1.0 wt%), but at higher concentrations (>2.0 wt%), the dispersion is

hindered by growing viscosity and agglomeration effects.

6. Conclusion

This thorough study was a systematic analysis of the synergistic behavior of carbon nanotube reinforcement, delamination size, stacked sequences and boundary conditions on the vibration properties of CFRP composite plates involving integrated analytical, numerical and experimental methods. The key conclusions can be summarized as follows:

1. Incorporation of carbon nanotube at 1.0 wt% concentration demonstrated 12-18 per cent improvement in natural frequencies in pristine CFRP composites and the magnitude of the improvement varied with stacking sequence. Layup with maximum enhancement (16.2) was attained in quasi-isotropic configurations because off-axis plies had higher contribution of matrix and moderate improvement was attained in cross-ply configurations (14.3) and angle-ply sequences (12.9). The mechanism of enhancement holds its work mainly on enhanced transverse modulus and interlaminar shear strength.

2. Under simply supported conditions, natural frequencies showed 36.6 percent reduction in 55 percent delamination in pristine CFRP compared to 28.5 percent in CNT-reinforced composites indicating 22 percent improvement in damage tolerance. This increased resistance is due to the CNT bridging mechanisms that increase interlaminar fracture and limit the delamination opening when vibrating.

3. Boundary conditions had a strong impact on absolute frequency magnitudes but the impact of delamination effects was fairly the same regardless of support configurations. The constraints clamped on were the highest frequency (163.0 Hz in intact CNT composite), then came simply supported (98.7 Hz) and free-free (47.3 Hz), with frequencies ratio of 1.65:1.00:0.48. Relative decreases caused by delamination were not very large (28.4-29.0%), which implies relatively independent processes.

4. The reinforcements of CNT yielded more homogeneous strain energy distributions and lowering stress concentration at delamination boundaries by 12-15% which resulted in increased damage tolerance. The values of modal assurance criterion of fundamental modes (0.96-0.98) of the intact and delaminated configurations of CNT composites demonstrated the strong similarity.

5. A good correlation was obtained between finite element results, analytical results obtained through Rayleigh-Ritz method, and experimental results. The computational frameworks were proved by finding mean absolute percentage error of 3.14% (FEA vs. experimental), 4.27% (analytical vs. experimental), and 1.89% (FEA vs. analytical). Frequencies were slightly over-predicted in both approaches (+2.1% FEA and +3.4% analytical) because of perfect bonding and a uniform rubric assumptions.

6. The quasi-isotropic stacking sequence [0/45/-45/90]n exhibited the best performance in terms of costly frequency to achieve high frequency with maximum CNT enhancement advantages as well as good damage tolerance, thus it is the best configuration to use in vibration sensitive application. The introduction of strategic CNT in the laminates made of matrices is less expensive to upgrade compared to fiber-dominated laminates. Future research directions are: (1) research on higher CNT loading fractions (1-3 wt%) using advanced dispersion methods, (2) research on non-uniform CNT distributions (functionally graded) to achieve desired properties (3) dynamic impact loading response of CNT composites, (4) long term durability under hygrothermal aging, and (5) multifunctional integration by taking advantage of the CNT electrical conductivity to structural health monitoring in addition to mechanical enhancement.

7. Acknowledgement

The author gratefully acknowledges the editorial office of Reports in Mechanical Engineering for granting a full waiver of the Article Processing Charge (APC).

References

Agarwal, B. D., Broutman, L. J., & Chandrashekhara, K. (2017). *Analysis and performance of fiber composites*. John Wiley & Sons. https://doi.org/10.1115/1.3157582

Agarwal, K., Kuchipudi, S. K., Girard, B., & Houser, M. (2018). Mechanical properties of fiber reinforced polymer composites: A comparative study of conventional and additive manufacturing methods. *Journal of Composite Materials*, *52*(23), 3173-3181. https://doi.org/10.1177/0021998318762297

Alexopoulos, N., Bartholome, C., Poulin, P., & Marioli-Riga, Z. (2010). Structural health monitoring of glass fiber

reinforced composites using embedded carbon nanotube (CNT) fibers. *Composites Science and Technology*, *70*(2), 260-271. https://doi.org/10.1016/j.compscitech.2009.10.017

Chakraborty, S., Singh, V., Dey, T., & Kumar, R. (2024). Influence of Carbon Nanotubes on Stability and Vibration Characteristics of Plates and Panels in Thermal Environment: A Review *Archives of Computational Methods in Engineering*, *31*(1), 147-178. https://doi.org/10.1007/s11831-023-09976-z

Coleman, J. N., Khan, U., Blau, W. J., & Gun'ko, Y. K. (2006). Small but strong: a review of the mechanical properties of carbon nanotube–polymer composites. *Carbon*, *44*(9), 1624-1652. https://doi.org/10.1016/j.carbon.2006.02.038

Das, S., & Sarangi, S. (2016). Static analysis of functionally graded composite beams. In *IOP Conference Series: Materials Science and Engineering* (Vol. 149, pp. 012138). IOP Publishing. https://doi.org/10.1088/1757-899X/149/1/012138

Fang, B., Chang, D., Xu, Z., & Gao, C. (2020). A review on graphene fibers: expectations, advances, and prospects. *Advanced materials*, *32*(5), 1902664. https://doi.org/10.1002/adma.201902664

Friedrich, K., & Almajid, A. A. (2013). Manufacturing aspects of advanced polymer composites for automotive applications. *Applied Composite Materials*, *20*(2), 107-128. https://doi.org/10.1007/s10443-012-9258-7

García-Macías, E., Castro-Triguero, R., Flores, E. I. S., Friswell, M. I., & Gallego, R. (2016). Static and free vibration analysis of functionally graded carbon nanotube reinforced skew plates. *Composite Structures*, *140*, 473-490. https://doi.org/10.1016/j.compstruct.2015.12.044

Garcia, C., Trendafilova, I., Zucchelli, A., & Contreras, J. (2018). The effect of nylon nanofibers on the dynamic behaviour and the delamination resistance of GFRP composites. In *MATEC Web of Conferences* (Vol. 148). https://doi.org/10.1051/matecconf/201814814001

Hassan, S. A., Santulli, C., Yahya, M. Y., Gang, C. L., & Abu Bakar, M. N. (2018). The potential of biomimetics design in the development of impact resistant material. *FME TRANSACTIONS*, *46*(1), 108-116. https://doi.org/10.5937/fmet1801108H

Iijima, S. (1991). Helical microtubules of graphitic carbon. *Nature*, *354*(6348), 56-58. https://doi.org/10.1038/354056a0

Kinloch, I. A., Suhr, J., Lou, J., Young, R. J., & Ajayan, P. M. (2018). Composites with carbon nanotubes and graphene: An outlook. *Science*, *362*(6414), 547-553. https://doi.org/10.1126/science.aat7439

Lei, Z., Zhang, L., & Liew, K. (2015). Free vibration analysis of laminated FG-CNT reinforced composite rectangular plates using the kp-Ritz method. *Composite Structures*, *127*, 245-259. https://doi.org/10.1016/j.compstruct.2015.03.019

Liew, K., Lei, Z., & Zhang, L. (2015). Mechanical analysis of functionally graded carbon nanotube reinforced composites: a review. *Composite Structures*, *120*, 90-97. https://doi.org/10.1016/j.compstruct.2014.09.041

Luo, H., & Hanagud, S. (2000). Dynamics of delaminated beams. *International Journal of Solids and Structures*, *37*(10), 1501-1519. https://doi.org/10.1016/S0020-7683(98)00325-4

Mehar, K., Panda, S. K., Dehengia, A., & Kar, V. R. (2016). Vibration analysis of functionally graded carbon nanotube reinforced composite plate in thermal environment. *Journal of Sandwich Structures & Materials*, *18*(2), 151-173. https://doi.org/10.1177/1099636215613324

Pingulkar, P., & Suresha, B. (2016). Free vibration analysis of laminated composite plates using finite element method. *Polymers and Polymer Composites*, *24*(7), 529-538. https://doi.org/10.1177/096739111602400712

Qian, D., Dickey, E. C., Andrews, R., & Rantell, T. (2000). Load transfer and deformation mechanisms in carbon nanotube-polystyrene composites. *Applied physics letters*, *76*(20), 2868-2870. https://doi.org/10.1063/1.126500

Rafiee, M., Nitzsche, F., & Labrosse, M. (2017). Dynamics, vibration and control of rotating composite beams and blades: A critical review. *Thin-Walled Structures*, *119*, 795-819. https://doi.org/10.1016/j.tws.2017.06.018

Ramanathan, T., Abdala, A., Stankovich, S., Dikin, D., Herrera-Alonso, M., Piner, R., Adamson, D., Schniepp, H., Chen, X., & Ruoff, R. (2008). Functionalized graphene sheets for polymer nanocomposites. *Nature nanotechnology*, *3*(6), 327-331. https://doi.org/10.1038/nnano.2008.96

Shen, H.-S. (2009). Nonlinear bending of functionally graded carbon nanotube-reinforced composite plates in thermal environments. *Composite Structures*, *91*(1), 9-19. https://doi.org/10.1016/j.compstruct.2009.04.026

Shen, M.-H., & Grady, J. (1992). Free vibrations of delaminated beams. *AIAA Journal*, *30*(5), 1361-1370. https://doi.org/10.2514/3.11072

Shokrieh, M. M., & Rafiee, R. (2010). Investigation of nanotube length effect on the reinforcement efficiency in carbon nanotube based composites. *Composite Structures*, *92*(10), 2415-2420. https://doi.org/10.1016/j.compstruct.2010.02.018

Spitalsky, Z., Tasis, D., Papagelis, K., & Galiotis, C. (2010). Carbon nanotube–polymer composites: chemistry, processing, mechanical and electrical properties. *Progress in polymer science*, *35*(3), 357-401. https://doi.org/10.1016/j.progpolymsci.2009.09.003

Thornburgh, R., & Chattopadhyay, A. (2002). Modeling the dynamic effects of delamination in adaptive composite laminate. In *43rd AIAA/ASME/ASCE/AHS/ASC Structures, Structural Dynamics, and Materials Conference* (pp. 1443). https://doi.org/10.2514/6.2002-1443

Thostenson, E. T., & Chou, T. W. (2006). Carbon nanotube networks: sensing of distributed strain and damage for life prediction and self healing. *Advanced materials*, *18*(21), 2837-2841. https://doi.org/10.1002/adma.200600977

Thostenson, E. T., Ren, Z., & Chou, T.-W. (2001). Advances in the science and technology of carbon nanotubes and their composites: a review. *Composites Science and Technology*, *61*(13), 1899-1912. https://doi.org/10.1016/S0266-3538(01)00094-X

Treacy, M. J., Ebbesen, T. W., & Gibson, J. M. (1996). Exceptionally high Young's modulus observed for individual carbon nanotubes. *Nature*, *381*(6584), 678-680. https://doi.org/10.1038/381678a0

Tsai, K. H., Hwan, C. L., Lin, M. J., Lo, C. C., & Hwang, J. L. (2017). Free vibration of braided composite plates with a center hole. . *Journal of the Chinese Society of Mechanical Engineers*, *38*(2), 135-144. https://tinyurl.com/bdebwkxr

Tseng, H.-C., Chang, R.-Y., & Hsu, C.-H. (2017). Numerical prediction of fiber orientation and mechanical performance for short/long glass and carbon fiber-reinforced composites. *Composites Science and Technology*, *144*, 51-56. https://doi.org/10.1016/j.compscitech.2017.02.020

Vo, T. P., Thai, H.-T., & Aydogdu, M. (2017). Free vibration of axially loaded composite beams using a four-unknown shear and normal deformation theory. *Composite Structures*, *178*, 406-414. https://doi.org/10.1016/j.compstruct.2017.07.022

Yu, M.-F., Files, B. S., Arepalli, S., & Ruoff, R. S. (2000). Tensile Loading of Ropes of Single Wall Carbon Nanotubes and their Mechanical Properties. *Physical Review Letters*, *84*(24), 5552-5555. https://doi.org/10.1103/PhysRevLett.84.5552

Zhang, H., Ibarra-Castanedo, C., Maldague, X., Sfarra, S., Perilli, S., Sarasini, F., Fernandes, H., Duan, Y., Peeters, J., & Avdelidis, N. (2018). Optical and mechanical excitation thermography for impact response in basalt-carbon hybrid fiber-reinforced composite laminates. *IEEE transactions on industrial informatics*, *14*(2), 514-522. https://doi.org/10.1109/TII.2017.2744179

Zhang, X., Zhao, N., & He, C. (2020). The superior mechanical and physical properties of nanocarbon reinforced bulk composites achieved by architecture design–a review. *Progress in Materials Science*, *113*, 100672. https://doi.org/10.1016/j.pmatsci.2020.100672

Zhang, Z., Shankar, K., Morozov, E. V., & Tahtali, M. (2016). Vibration-based delamination detection in composite beams through frequency changes. *Journal of Vibration and Control*, *22*(2), 496-512. https://doi.org/10.1177/1077546314533584

Zou, Y., Tong, L., & Steven, G. P. (2000). Vibration-based model-dependent damage (delamination) identification and health monitoring for composite structures—a review. *Journal of sound and vibration*, *230*(2), 357-378. https://doi.org/10.1006/jsvi.1999.2624